ACS APPLIED MATERIALS & INTERFACES

Research Article

www.acsami.org

Effect of Water Vapor on Pd-Loaded SnO_2 Nanoparticles Gas Sensor

Nan Ma,[†] Koichi Suematsu,[‡] Masayoshi Yuasa,[‡] Tetsuya Kida,[§] and Kengo Shimanoe*[,‡]

[†]Interdisciplinary Graduate School of Engineering Sciences and [‡]Faculty of Engineering Sciences, Kyushu University, Fukuoka 816-8580, Japan

[§]Department of Applied Chemistry and Biochemistry, Kumamoto University, Kumamoto 860-8555, Japan

ABSTRACT: The effect of water vapor on Pd-loaded SnO_2 sensor was investigated through the oxygen adsorption behavior and sensing properties toward hydrogen and CO under different humidity conditions. On the basis of the theoretical model reported previously, it was found that the mainly adsorbed oxygen species on the SnO_2 surface in humid atmosphere was changed by loading Pd, more specifically, for neat SnO_2 was O^-, while for 0.7% Pd-SnO_2 was O^{2-}. The water vapor poisoning effect on electric resistance and sensor response was reduced by loading Pd. Moreover the sensor response in wet atmosphere was greatly enhanced by loading Pd. It seems that the electron depletion layer by p−n junction of PdO-SnO_2 may impede OH^- adsorption.

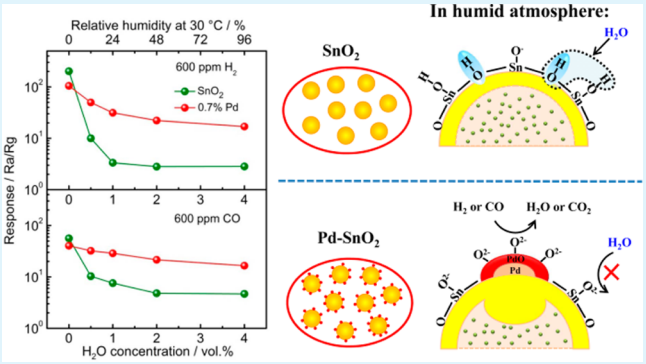

KEYWORDS: *SnO_2 nanoparticles, Pd loading, water vapor, oxygen adsorption, H_2, CO*

INTRODUCTION

Tin dioxide (SnO_2) has been extensively studied as a gas-sensing material for almost half a century.[1] It is widely used for detecting reducing (H_2 and CO) and oxidizing (NO_2 and O_3) gases. As one of the most important considerations in the practical use of sensors, humidity deteriorates the sensitivity of sensor seriously.[2−4] Even though many corresponding researches have been performed to explain this phenomenon to further reduce the water vapor poisoning effect on the sensor performance,[5−7] the reaction mechanisms of how the water vapor interferes with the detection of the target gas are still not yet clarified in detail.

A high sensor response is closely related to the adsorbed oxygen species on the SnO_2 surface. Oxygen adsorption species as O^- and O^{2-} can be written as follows:

$$O_2 + 2e^- = 2O^- \quad \text{(R1)}$$

$$O_2 + 4e^- = 2O^{2-} \quad \text{(R2)}$$

Theoretical model and formulas were proposed based on the power laws in case of spherical SnO_2.[8] The relationship between the electric resistance and oxygen partial pressure was formulated by combining the depletion model as well as oxygen adsorption and reaction. This can be expressed as follows in terms of the adsorbed oxygen species O^- and O^{2-}:

$$\frac{R}{R_0} = \frac{3}{a}(K_1 P_{O2})^{1/2} + c\ (O^- \text{ formation}) \quad (1)$$

$$\frac{R}{R_0} = \left\{\frac{1}{4}(c(n))^2 + \left(\frac{6N_D}{a}\right)(K_2 P_{O2})^{1/2}\right\}^{1/2} + c\ (O^{2-} \text{ formation}) \quad (2)$$

Here R_0 is the electric resistance at flat-band condition, a is the grain radius, c is a constant, N_D is the donor density, K_1 and K_2 are equilibrium constants of adsorption. Yamazoe et al.[3,8] proposed that O^{2-} was mainly adsorbed on the SnO_2 surface in dry atmosphere, and the electric resistance was linearly proportional to $P_{O2}{}^{1/4}$. However, in the case of wet atmosphere, O^{2-} was completely blocked by water vapor, leaving O^- on the SnO_2 surface. Therefore, the electric resistance showed a linear relationship to $P_{O2}{}^{1/2}$. The oxygen species was influenced by water vapor, resulting in the decrease of sensor response in wet atmosphere.

The sensor response to hydrogen was also mentioned in dry and wet atmosphere, which was defined by the following equations:[3]

$$H_2 + O^- = H_2O + e^- \quad \text{(R3)}$$

$$H_2 + O^{2-} = H_2O + 2e^- \quad \text{(R4)}$$

$$\frac{Ra}{Rg} = \left(\frac{3c}{aN_D}\right)^{1/2} \cdot P_{H2}{}^{1/2} + \text{const (in wet atmosphere)} \quad (3)$$

Received: December 24, 2014
Accepted: March 3, 2015
Published: March 3, 2015

DOI: 10.1021/am509082w
ACS Appl. Mater. Interfaces 2015, 7, 5863−5869

$$\frac{Ra}{Rg} = f\left(\frac{3(k_2/k_{-1})}{aN_D}\right)^{1/2} \cdot {P_{H2}}^{1/2} \text{ (in dry atmosphere)} \quad (4)$$

Here Ra and Rg are the electrical resistances in air and hydrogen gas, respectively, k_2 and k_{-1} are the rate constants of forward and reverse reaction of R1, P_{H2} is the hydrogen partial pressure, and f is an amplifying factor. The sensor response is proportional to ${P_{H2}}^{1/2}$ in both dry and wet atmosphere for neat SnO_2.

It is well-known that palladium (Pd) is one of the most effective receptors not only for enhancing the sensitivity but also for suppressing the water vapor poisoning.[6,7,9] Two mechanisms are mainly proposed toward the role of Pd in the sensing process, namely, the chemical and electronic effects.[10] The former is focused on the ability of Pd to activate the target gas and to facilitate its catalytic oxidation on the SnO_2 surface. The latter considers that conductance change due to the variation of contact potential between Pd and SnO_2 interface by the oxidation state change of Pd.[11] However, the suppression effect of Pd on water vapor poisoning is still under discussion. Koziej suggested that Pd was dispersed at an atomic level on the SnO_2 surface, and Pd could provide initial adsorption sites for oxygen species adsorption.[12] Pavelko proposed that the presence of Pd changed the reaction partner for hydrogen with water vapor. For SnO_2, hydrogen reacts with water through bridging hydroxyl groups, whereas Pd-loaded SnO_2 interacts with hydrogen and water through bridging oxygen.[7]

In this paper, on the basis of these theories, we investigated the oxygen adsorption behavior of SnO_2 and Pd-loaded SnO_2 (0.7% Pd-SnO_2) in different humid atmospheres and confirmed the adsorbed oxygen species by power laws. Additionally the sensor response to H_2 and CO was studied in dry and wet atmospheres.

■. EXPERIMENTAL SECTION

Synthesis of Pd-Loaded SnO_2 Nanoparticles. SnO_2 nanoparticles were synthesized by following precipitation route. $SnCl_4 \cdot 5H_2O$ aqueous solution was slowly dropped into NH_4HCO_3 solution with stirring. The resulting precipitate was centrifuged and washed with NH_4NO_3 solution several times to remove Cl^- ions, and then hydrothermally treated in an ammonia solution (pH = 10.5) under the pressure of 10 MPa at 200 °C for 3 h. The SnO_2 sol was dried at 120 °C and then heat-treated at 600 °C in oxygen atmosphere. To load Pd particles on SnO_2 surface, SnO_2 powder was impregnated with $Pd(NH_3)_2(NO_2)_2$ aqueous solution, followed by ammonia solution treatment (pH = 9.5), filtration, drying at 120 °C, and heat treatment at 500 °C in air.

Material Characterization. The loading amount of Pd was determined by energy-dispersive X-ray fluorescence spectrometer (XRF, EDX-800, Shimadzu, Japan). The crystal structure of powders was analyzed by X-ray diffraction with copper Kα radiation (λ = 1.5418 Å) filtered through a Ni foil (XRD, RINT 2100, Rigaku, Japan). Specific surface area and peak pore radius were measured by surface area analyzer (BET, Belsorp, BEL Japan). The microstructure was observed by transmission electron microscopy (TEM) and high resolution TEM (HRTEM) (Tecnai-F20, FEI, US).

CO pulse adsorption method was used to decide the particle size, dispersion state, and Pd surface area on SnO_2 in this study (BEL-CAT, BEL Japan), which is one of the most effective methods to investigate the distribution state of catalyst on supporting material.[13−15] It was conducted on the quartz tube reactor, and the effluent gas was monitored by online quadrupole mass spectroscopy. Powders (25 mg) were pretreated at 400 °C for 5 min in a flow of air, and then cooled to 40 °C. After exposing to He for 5 min, the sample was heated to 80 °C in a flow of 5% H_2/N_2 followed by flushing with He for 10 min. Then 1% CO/N_2 was pulse-injected into the reactor system after the temperature was reduced to 40 °C. The stoichiometry of one CO molecule per one Pd atom on the surface of Pd particle was used for the calculation of Pd dispersion. The Pd particle size was calculated by using the equation $d = 6V/S$, where V and S indicate the volume and surface area of palladium, respectively. In this experiment, CO pulse adsorption measurement was also conducted on neat SnO_2. It was found that no CO adsorbed on the surface of neat SnO_2.

The temperature-programmed reduction (TPR) measurement was carried out with 1000 ppm H_2/N_2 and CO/N_2, respectively. Prior to the experiment, 50 mg of powder was calcined at 400 °C for 30 min with a heating rate of 10 °C/min in air, then cooled to 50 °C. After the powder was He-purged for 10 min, the TPR experiment was performed with H_2/N_2 and CO/N_2 respectively, the temperature being increased from 50 to 500 °C with a ramp rate of 10 °C/min. Thermal conductivity detector (TCD) and mass spectrometer (MS) were employed to monitor the H_2 consumption, H_2O, and CO_2 emission.

Sensor Fabrication and Measurement. Sensing films were prepared as follows. The obtained powders were mixed with appropriate amount of α-terpineol to form uniform paste, and then screen-printed on an alumina substrate ($9 \times 13 \times 0.38$ mm^3) attached with Au electrodes (line width: 180 μm, distance between lines: 90 μm, sensing area: 64 mm^2). The resulting devices were heat-treated at 580 °C for 3 h in air to remove the organic binder and stabilize the sensing layer.

The measurements were carried out in a conventional gas flow apparatus equipped with an electric furnace. Before sensing test, gases (air, O_2, and N_2) were pretreated by catalyst Pt/Al_2O_3 and zeolite to remove impurity gases (such as CO and hydrocarbon) and water, respectively. The water vapor was controlled strictly by using a set of humidity supplier and humidity sensor system. Oxygen sensor (zirconia oxygen cell) was used to measure the oxygen partial pressure. A multimeter (model 2701, Keithley Instruments Inc.) was connected to the sensor to monitor electric resistance. Prior to measurement, sensors were pretreated at 580 °C for 1 h in dry atmosphere to eliminate the impurities that adsorbed at low temperature. To reach to an equilibrium of water vapor adsorption, the sensors were treated at 580 °C for 2 h after introducing water vapor (4 vol % H_2O), and then the temperature was reduced gradually to 300 or 350 °C. The detailed pretreatment process is shown in Figure 1. The electric resistance was measured under the flow of 80

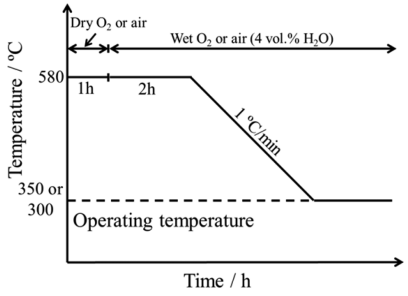

Figure 1. Pretreated process before sensing properties measurement.

cm^3/min in different humidity (0−4 vol % H_2O). The sensor response (S) was defined as the ratio of electric resistance in synthetic air (Ra) to that in hydrogen gas (Rg).

■. RESULTS AND DISCUSSION

Characterization of Material. Figure 2 shows the Pd loading amount as a function of precursor concentration. The Pd loading amount reached a saturation level when the precursor concentration increased to 0.7 mol %. This precursor solution gives a very small Pd particle, as mentioned later, but the Pd particles seem to disperse in solution because the

DOI: 10.1021/am509082w
ACS Appl. Mater. Interfaces 2015, 7, 5863−5869

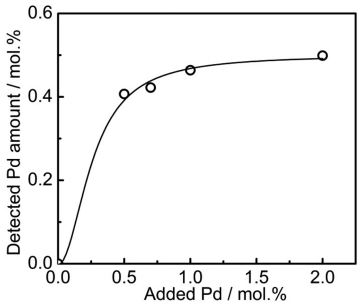

Figure 2. Pd loading amount as a function of the precursor concentration.

adhesion to SnO_2 surface is weak. Therefore, most of the Pd species was dispersed in solution when the Pd precursor concentration was 0.7 mol % excess, and it was removed by the filtration process. Figure 3 shows the XRD patterns of SnO_2

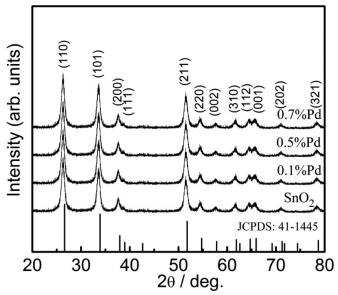

Figure 3. X-ray diffraction patterns of SnO_2 and Pd-loaded SnO_2.

and Pd-loaded SnO_2 (0.1, 0.5, 0.7 mol %). It was demonstrated that all the samples exhibited a same tetragonal phase (JCPDS: 41−1445). No phase corresponding to Pd or PdO was detected in the Pd-loaded SnO_2 powders due to extremely low Pd amount.

Figure 4 is the TEM images of SnO_2 and 0.7% Pd-SnO_2. Clearly, Pd-loaded SnO_2 maintained the same morphology as neat SnO_2 particles. The particle size of SnO_2 and 0.7% Pd-SnO_2 was almost same, ca. 14 nm. The interplanar spacing of 0.34 and 0.26 nm corresponded to $(01\bar{1})$ and $(\bar{1}0\bar{1})$ planes in a tetragonal SnO_2 structure, respectively. The fast Fourier transform pattern indicated a good single-crystalline quality. However, no Pd or PdO clusters were directly observed by HRTEM, even when the Pd loading amount reached 0.7 mol %. Because the Pd loading amount was extremely low, it is presumed that no large Pd or PdO cluster was formed on the SnO_2 surface. It has been reported that Pd tends to form clusters of PdO on the SnO_2 surface if Pd-loaded SnO_2 powder was prepared by the wet impregnating method.[16] On the other hand, the atomic numbers of Pd and Sn are very close (46 and 50, respectively), which leads to a difficulty in distinguishing the Pd phase on the SnO_2 background.[17] To overcome such difficulty, Pd characteristics on SnO_2 surface were investigated by CO pulse chemisorption method. Table 1 shows particle size, distribution, and surface area of Pd on SnO_2 for 0.7% Pd-loaded SnO_2. It was found that calculated particle size of Pd was 2.59 nm, and the particles were finely dispersed on the surface of SnO_2.

Table 1. Specific Surface Area of SnO_2 and 0.7% Pd-SnO_2, as well as Pd Amount, Particle Size, Dispersion and Surface Area of Pd on SnO_2 for 0.7% Pd-SnO_2

sample	specific surface area (m^2/g)	Pd amount (mol %)	particle size of Pd (nm)	dispersion of Pd (%)[a]	surface area of Pd (m^2/g)
SnO_2	27.1				
0.7% Pd-SnO_2	27.1	0.42	2.59	43.2	0.65

[a]Dispersion of Pd was defined as the ratio of Pd atoms available for CO chemisorption to the total Pd atoms.

The crystallite size, specific surface area, and peak pore radius of SnO_2 and Pd-loaded SnO_2 powders are summarized in Table 2. It was found that Pd had no significant effect on the SnO_2 crystallite size. The crystallite sizes calculated from the (110) peak by Scherrer equation were almost same for SnO_2 and Pd-SnO_2 powders, ~12 nm. Furthermore, the specific surface area and peak pore radius of all the powders had not much difference. It is well-known that the morphology of powders, especially the crystallite size, influences the sensor response

Table 2. Average Crystallite Size, Specific Surface Area, and Peak Pore Radius for Neat SnO_2 and Pd-Loaded SnO_2

sample	average crystallite size (nm)	specific surface area (m^2/g)	peak pore radius (nm)
SnO_2	11.7	27.1	9
0.1% Pd-SnO_2	11.9	28.3	8
0.5% Pd-SnO_2	11.6	27.8	9
0.7% Pd-SnO_2	11.8	27.1	8

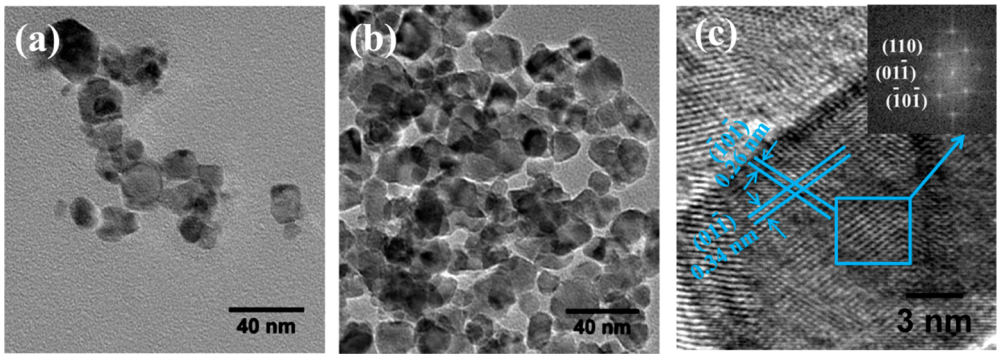

Figure 4. TEM images of SnO_2 (a) and 0.7% Pd-SnO_2 (b); HRTEM image of 0.7% Pd-SnO_2 (c); the fast Fourier transform (inset).

DOI: 10.1021/am509082w
ACS Appl. Mater. Interfaces 2015, 7, 5863−5869

more greatly.[18] On the basis of above results, it was found that Pd loading did not change the morphology of SnO_2. Thus, we can eliminate the influence of morphology to the sensor response and only focus on the effect of Pd on the sensing properties.

Oxygen Adsorption Behavior in Different Humidity. Figure 5 shows the electric resistance change with water vapor

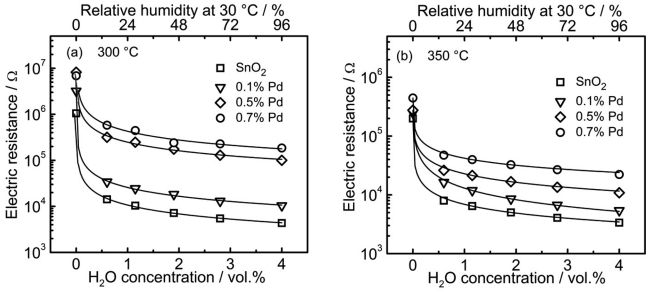

Figure 5. Electric resistance in different humid air for neat SnO_2 and Pd-loaded SnO_2 at 300 °C (a) and 350 °C (b).

concentration in air at 300 and 350 °C. The electric resistance of all the sensors was reduced drastically in the presence of small amount of water vapor. However, the change tended to become small at 350 °C. As for it, it is thought that the surface hydroxyl group is desorbed at 350 °C as shown in the report of Yamazoe.[19] Interestingly, the electric resistances of 0.7% Pd-SnO_2 were ~40 and 6 times higher than those of neat SnO_2 at 300 and 350 °C, respectively, in wet atmosphere. Obviously, the reduction of electric resistance in wet atmosphere was effectively suppressed by loading Pd. Additionally, the electric resistance was increased with raising Pd loading amount in wet atmosphere. So far, it is well-known that Pd loading on SnO_2 gives high electric resistance and sensor response because of electronic sensitization by junction of p-type PdO and n-type SnO_2.[20] However, the effect in wet atmosphere is not clarified enough. Therefore, on the basis of the results, neat SnO_2 and 0.7% Pd-SnO_2 sensors were used to investigate the oxygen adsorption behavior and sensor response to H_2 and CO in different humidity.

Figure 6 shows the dependence of electric resistance on oxygen partial pressure at 300 °C in dry and wet atmospheres. In dry atmosphere, the electric resistances of both neat SnO_2 and 0.7% Pd-SnO_2 were linearly proportional to $P_{O2}^{1/4}$ in the measured range (Figure 6b). Such a linear relationship agreed with the theoretical eq 2, indicating the adsorbed oxygen species was O^{2-}. However, with increasing humidity to 0.5 vol % H_2O (Figure 6c,d), the dependence of electric resistance on oxygen partial pressure was changed for neat SnO_2. And the electric resistance was linearly proportional to $P_{O2}^{1/2}$, meaning that the oxygen adsorption species was changed from O^{2-} to O^- in wet atmosphere. The results were in agreement with the previous report for neat SnO_2.[8] O^{2-} was only formed in dry atmosphere, and it was strongly suppressed by adsorbed OH^- group even in low-humidity atmosphere, thus leaving O^- as the mainly adsorbed oxygen species. On the other hand, oxygen adsorption behavior for 0.7% Pd-SnO_2 sensor in humidity of 0.5 vol % H_2O was completely different from those for neat SnO_2; that is, a linear proportion of electric resistance to $P_{O2}^{1/4}$ was observed. It seems the mainly adsorbed oxygen species had no change from dry to wet atmosphere, adsorbing as O^{2-}. In high humidity of 4 vol % H_2O (Figure 6e,f), SnO_2 and 0.7% Pd-

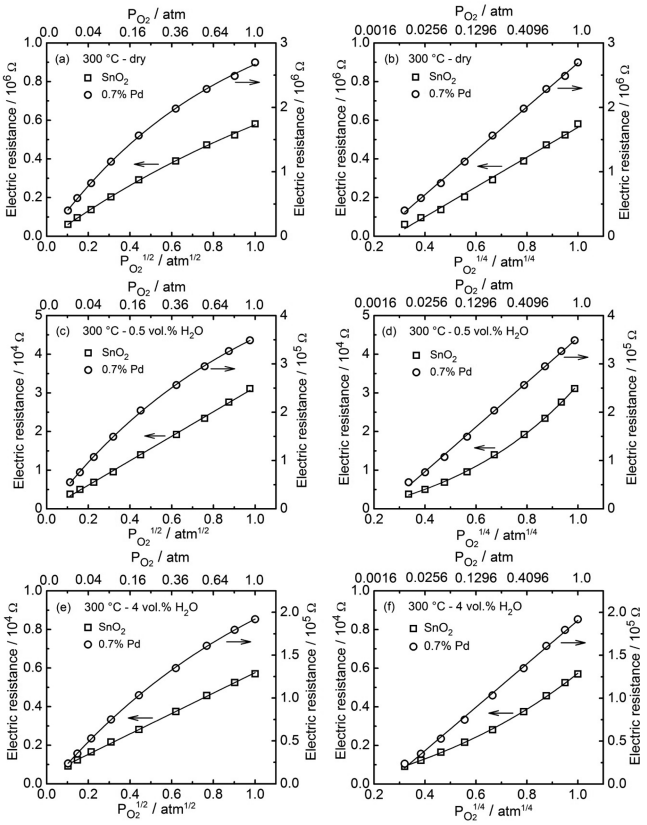

Figure 6. Dependence of the electric resistance on the $P_{O2}^{1/4}$ and $P_{O2}^{1/2}$ at 300 °C: (a, b) dry; (c, d) 0.5 vol % H_2O; (e, f) 4 vol % H_2O.

SnO_2 showed the same oxygen adsorption behavior as that in humidity of 0.5 vol % H_2O. In addition, such a behavior of electrical resistance to oxygen partial pressure was observed even at 350 °C as shown in Figure 7. From these results, it seems the sensing model at 350 °C is almost same as that at 300 °C although the degree of change in electric resistance under humid condition is different.

Sensor Response to H_2 and CO in Different Humidity. The sensor response to 600 ppm of H_2 and CO in different humidity at 300 and 350 °C is shown in Figure 8. In dry atmosphere, neat SnO_2 showed maximum sensor response to H_2 and CO at both 300 and 350 °C because such inflammable gases directly combusted on the surface of thick film by catalyzing of Pd at high temperature and did not diffuse into the vicinity of the electrode.[21−23] With increase in operating temperature to 350 °C, such oxidation becomes active, and the sensor response to H_2 even for neat SnO_2 deteriorated. However, the sensor response to CO for neat SnO_2 increased with increase in operating temperature because of the reaction activity different from H_2. On the other hand, the response to CO for 0.7% Pd-SnO_2 did not increase but rather slightly decreased by increasing temperature. This behavior also seems to be due to catalytic activity of Pd. However, the most interesting characteristic is sensor response under humid condition. The sensor response of both SnO_2 and 0.7% Pd-SnO_2 was reduced in the presence of small amount of water vapor, but the reduction level of sensor response for 0.7% Pd-SnO_2 in wet atmosphere was significantly different from that of neat SnO_2. The sensor response to H_2 and CO decreased seriously for neat SnO_2 in wet atmosphere, whereas H_2 response decreased only 3 times, and CO response decreased

DOI: 10.1021/am509082w
ACS Appl. Mater. Interfaces 2015, 7, 5863−5869

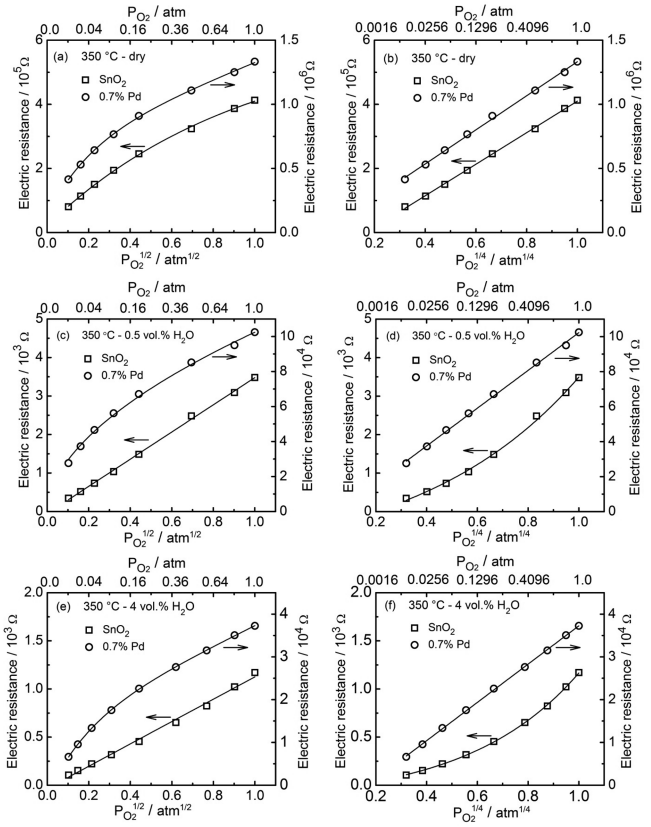

Figure 7. Dependence of the electric resistance on the $P_{O2}^{1/4}$ and $P_{O2}^{1/2}$ at 350 °C: (a, b) dry; (c, d) 0.5 vol % H_2O; (e, f) 4 vol % H_2O.

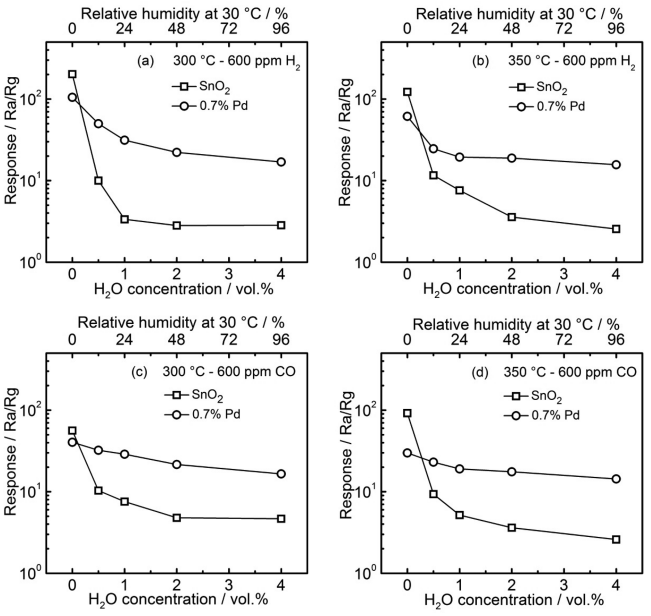

Figure 8. Sensor response to 600 ppm H_2 (a, b) and 600 ppm CO (c, d) for SnO_2 and 0.7% Pd-SnO_2 in different humidity at 300 and 350 °C.

even lower by loading Pd. In addition, the changes of sensor response in the range of 0.5 to 4 vol % H_2O were very small for 0.7% Pd-SnO_2, especially in the case operated at 350 °C. Obviously, Pd loading inhibited the decrease of sensor response in wet atmosphere, resulting in a much higher sensor response for 0.7% Pd-SnO_2.

Figures 9 and 10 show the square of the sensor response as a function of H_2 and CO partial pressure for neat SnO_2 and 0.7% Pd-SnO_2 in different humidity atmosphere. According to the theoretical eqs 3 and 4, the square of sensor response to H_2 and

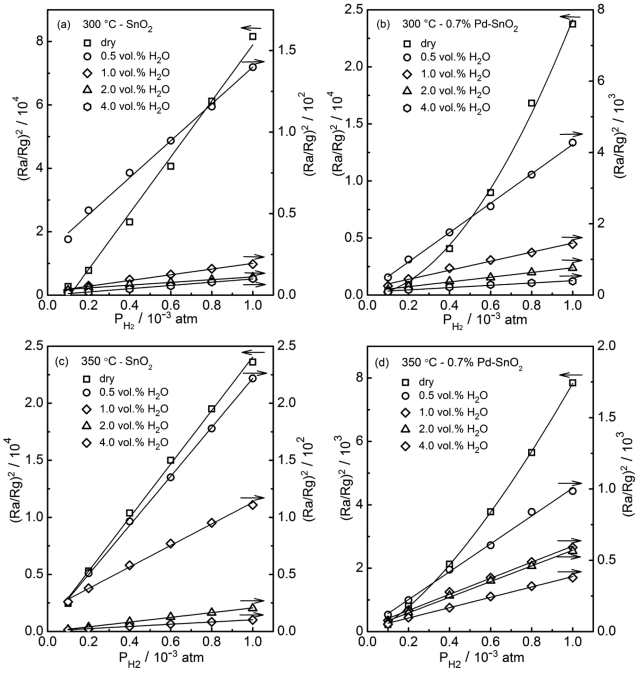

Figure 9. Relationship between the sensor response and the hydrogen partial pressure for SnO_2 and 0.7% Pd-SnO_2 at 300 °C (a, b) and 350 °C (c, d) in different humidity.

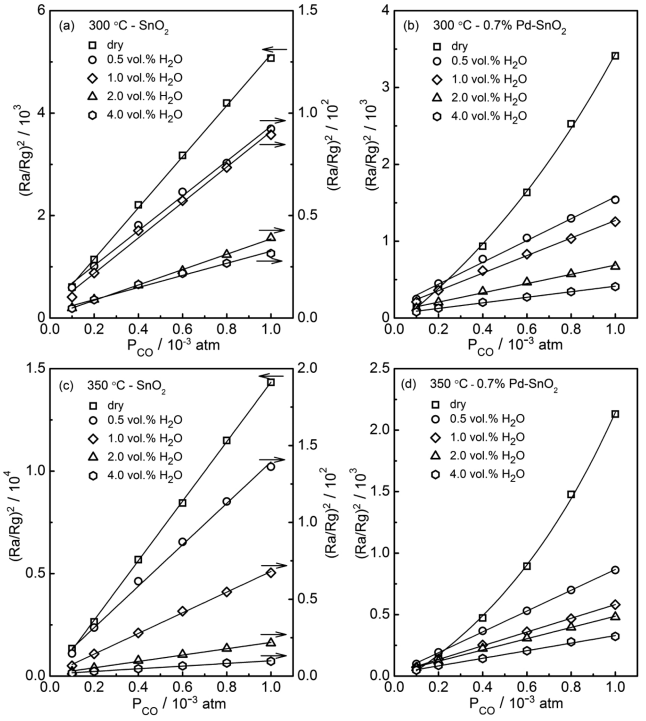

Figure 10. Relationship between the sensor response and the CO partial pressure for SnO_2 and 0.7% Pd-SnO_2 at 300 °C (a, b) and 350 °C (c, d) in different humidity.

DOI: 10.1021/am509082w
ACS Appl. Mater. Interfaces 2015, 7, 5863−5869

CO should have the linear relationship with the gas partial pressure for neat SnO_2 and 0.7% Pd-SnO_2 in both dry and wet atmosphere. In Figure 9a,c, a good linearity of $(Ra/Rg)^2$ to the P_{H2} was observed for neat SnO_2 in both dry and wet atmosphere, which was in agreement with eqs 3 and 4. H_2 reacted with adsorbed oxygen species O^{2-} and O^- as reported previously.[8] On the other hand, 0.7% Pd-SnO_2 sensor showed a nonlinear fit of $(Ra/Rg)^2$ with P_{H2} in dry atmosphere although it showed a good linearity of $(Ra/Rg)^2$ to the P_{H2} in wet atmosphere. Such behavior was observed for not only H_2 but also CO, as shown in Figure 10. Currently the reason why a nonlinear fit of $(Ra/Rg)^2$ with P_{H2} in dry atmosphere occurs is not well understood, but it is supposed that reactivity of PdO is related to such behavior. The details should be investigated more. For 0.7% Pd-SnO_2, the important point is that an adsorption species such as O^{2-} exists under humid conditions.

Temperature-Programmed Reduction Measurements of Neat SnO_2 and Pd-Loaded SnO_2. To investigate any difference in reactivity between neat SnO_2 and 0.7% Pd-SnO_2, TPR was carried out. Figure 11 shows H_2O desorption and H_2

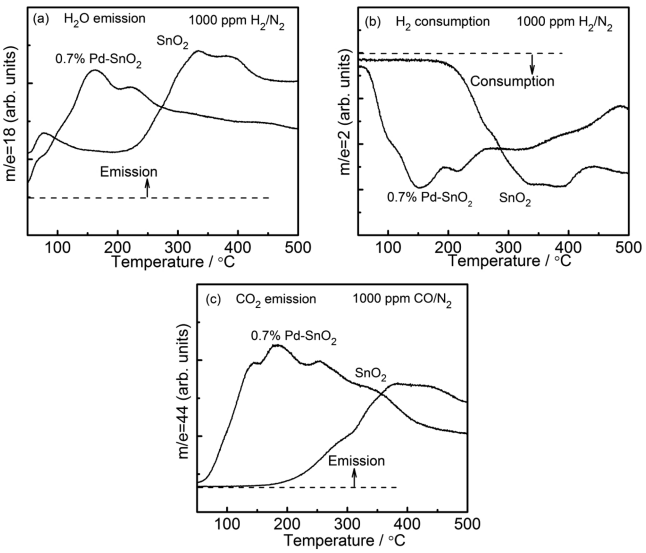

Figure 11. (a) H_2O desorption spectra and (b) H_2 consumption spectra of H_2-TPR and (c) CO_2 emission spectra of CO-TPR for neat SnO_2 and Pd-loaded SnO_2.

consumption spectra of H_2-TPR and CO_2 emission spectra of CO-TPR for neat SnO_2 and 0.7% Pd-SnO_2. H_2O desorption and H_2 consumption spectra for 0.7% Pd-SnO_2 are different from those for neat SnO_2. In the case of neat SnO_2, large peak was observed in the range of 300−400 °C. This peak seems to be due to O^{2-} and O^- adsorbed on SnO_2 surface as reported previously.[19] However, 0.7% Pd-SnO_2 showed two large peaks at 180 and 250 °C. Additionally, a slight and gentle peak was also observed above 300 °C. In the emission spectra of CO-TPR, the point different from H_2-TPR was to show a peak at 300 °C although other peaks shifted a little to lower temperature. The peak may be considered by partial reduction of SnO_2 surface because SnO_2 surface is reduced catalytically by Pd under CO existence.[24] From these results, it is thought that two kinds of oxygen species are related to Pd. One is O^{2-} adsorbed on PdO, and another is PdO itself. Furthermore, it seems that small amount of oxygen adsorbs on SnO_2 surface.

Model of Oxygen Adsorption on Pd-Loaded SnO_2 under Humid Condition. Schematic drawing of gas-sensing model for Pd-loaded SnO_2 in humid atmosphere is shown in Figure 12, as compared with that for neat SnO_2. In the case of

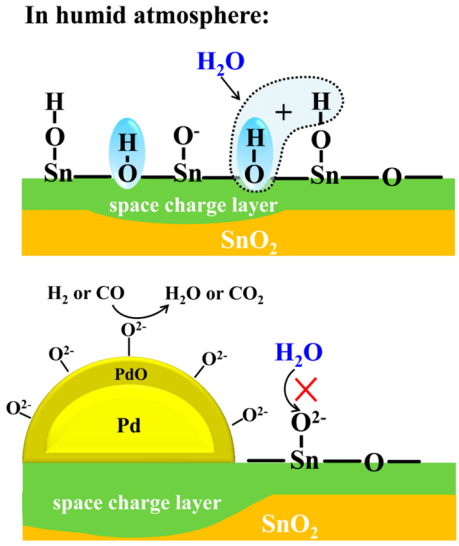

Figure 12. Schematic drawing of gas-sensing model for neat SnO_2 and Pd-loaded SnO_2 in humid atmosphere.

neat SnO_2, under humid condition, the OH^- groups competitively adsorb on the SnO_2 surface, and O^{2-} adsorption is disturbed by OH^-. From the results of the dependence of electric resistance on oxygen partial pressure, mainly oxygen species adsorbed in humid atmosphere may be estimated as O^- for neat SnO_2. However, such disturbance by water vapor was also inhibited by loading Pd. Pd existing as PdO is dispersed finely on SnO_2 surface as shown in Table 1. On the basis of the results of the dependence of electric resistance on oxygen partial pressure and the TPR, the assumption of O^{2-} adsorption is brought out. In addition, as one possibility, PdO may provide initial adsorption sites for O^{2-} adsorption, which is hard to be affected by water vapor. Such O^{2-} adsorption on PdO seems to let the depletion layer of the interface expand more and may prevent OH^- adsorption on SnO_2 surface.

CONCLUSION

The suppression effect of Pd on water vapor poisoning in Pd-loaded SnO_2 gas sensor was clarified with regard to oxygen adsorption behavior and gas-sensing properties toward reducing gas (H_2 and CO) in humid atmosphere. The following conclusions are drawn from the present study.

1. The adsorbed oxygen species on Pd-loaded SnO_2 surface was mainly O^{2-} both in dry and humid atmosphere, and the oxygen adsorption was not influenced by water vapor. However, for neat SnO_2, it was adsorbed as O^{2-} in dry atmosphere but changed to O^- in humid atmosphere.
2. The water vapor poisoning effect on electric resistance and sensor response was significantly reduced by loading Pd in humid atmosphere.
3. On the basis of the dependence of electric resistance on oxygen partial pressure and the TPR results, we propose that O^{2-} adsorption on PdO enlarged the depletion layer of the interface and prevented OH^- adsorption on SnO_2 surface.

DOI: 10.1021/am509082w
ACS Appl. Mater. Interfaces 2015, 7, 5863−5869

AUTHOR INFORMATION

Corresponding Author

*E-mail: shimanoe.kengo.695@m.kyushu-u.ac.jp.

Notes

The authors declare no competing financial interest.

REFERENCES

(1) Seiyama, T.; Kato, A.; Fujiishi, K.; Nagatani, M. A New Detector for Gaseous Components Using Semiconductive Thin Films. *Anal. Chem.* **1962**, *34*, 1502−1503.

(2) Barsan, N.; Weimar, U. Understanding the Fundamental Principles of Metal Oxide Based Gas Sensors; the Example of CO Sensing with SnO_2 Sensors in the Presence of Humidity. *J. Phys.: Condens. Matter* **2003**, *15*, 813−839.

(3) Yamazoe, N.; Suematsu, K.; Shimanoe, K. Extension of Receptor Function Theory to Include Two Types of Adsorbed Oxygen for Oxide Semiconductor Gas Sensors. *Sens. Actuators, B* **2012**, *163*, 128−135.

(4) Choi, K.; Hubner, M.; Haensch, A.; Kima, H. J.; Weimar, U.; Barsan, N.; Lee, J. H. Ambivalent Effect of Ni Loading on Gas Sensing Performance in SnO_2 Based Gas Sensor. *Sens. Actuators, B* **2013**, *183*, 401−410.

(5) Yamazoe, N.; Suematsu, K.; Shimanoe, K. Two Types of Moisture Effects on the Receptor Function of Neat Tin Oxide Gas Sensor to Oxygen. *Sens. Actuators, B* **2013**, *176*, 443−452.

(6) Harbeck, S.; Szatvanyi, A.; Barsan, N.; Weimar, U.; Hoffmann, V. DRIFT Studies of Thick Film Un-doped and Pd-Doped SnO_2 Sensors: Temperature Changes Effect and CO Detection Mechanism in the Presence of Water Vapour. *Thin Solid Films* **2003**, *436*, 76−83.

(7) Pavelko, R.; Daly, H.; Hardacre, C.; Vasilieva, A.; Llobeta, E. Interaction of Water, Hydrogen and Their Mixtures with SnO_2 Based Materials: the Role of Surface Hydroxyl Groups in Detection Mechanisms. *Phys. Chem. Chem. Phys.* **2010**, *12*, 2639−2647.

(8) Yamazoe, N.; Suematsu, K.; Shimanoe, K. Gas Reception and Signal Transduction of Neat Tin Oxide Semiconductor Sensor for Response to Oxygen. *Thin Solid Films* **2013**, *548*, 695−702.

(9) Koziej, D.; Barsan, N.; Shimanoe, K.; Yamazoe, N.; Szuber, J.; Weimar, U. Spectroscopic Insights into CO Sensing of Undoped and Palladium Doped Tin Dioxide Sensors Derived from Hydrothermally Treated Tin Oxide Sol. *Sens. Actuators, B* **2006**, *118*, 98−104.

(10) Yamazoe, N. New Approaches for Improving Semiconductor Gas Sensors. *Sens. Actuators, B* **1991**, *5*, 7−19.

(11) Safonova, O.; Neisius, T.; Ryzhikov, A.; Chenevier, B.; Gaskov, A.; Labeau, M. Characterization of the H_2 Sensing Mechanism of Pd-Promoted SnO_2 by XAS in Operando Conditions. *Chem. Commun.* **2005**, *41*, 5202−5204.

(12) Koziej, D.; Hubner, M.; Barsan, N.; Weimar, U.; Sikoraz, M.; Grunwaldt, J. Operando X-ray Absorption Spectroscopy Studies on Pd-SnO_2 Based Sensors. *Phys. Chem. Chem. Phys.* **2009**, *11*, 8620−8625.

(13) Kimura, K.; Einaga, H.; Teraoka, Y. Preparation of Highly Dispersed Platinum Catalysts on Various Oxides by Using Polymer-Protected Nanoparticle. *Catal. Today* **2011**, *164*, 88−91.

(14) Einaga, H.; Kawarada, J.; Kimura, K.; Teraoka, Y. Preparation of Platinum Nanoparticles on TiO_2 from DNA-Protected Particles. *Colloids Surf., A* **2014**, *455*, 179−184.

(15) Einaga, H.; Urahama, N.; Tou, A.; Teraoka, Y. CO Oxidation over TiO_2-Supported Pt−Fe Catalysts Prepared by Coimpregnation Methods. *Catal. Lett.* **2014**, *144*, 1653−1660.

(16) Cerda Belmonte, J.; Manzano, J.; Arbiol, J.; Cirera, A.; Puigcorbe, J.; Vila, A.; Sabate, N.; Gracia, I.; Cane, C.; Morante, J. R. Micromachined Twin Gas Sensor for CO and O_2 Quantification Based on Catalytically Modified Nano-SnO_2. *Sens. Actuators, B* **2006**, *114*, 881−892.

(17) Marikutsa, A.; Rumyantseva, M.; Yashina, L.; Gaskov, A. Role of Surface Hydroxyl Groups in Promoting Room Temperature CO Sensing by Pd-Modified Nanocrystalline SnO_2. *J. Solid State Chem.* **2010**, *183*, 2389−2399.

(18) Xu, C.; Tamaki, J.; Miura, N.; Yamazoe, N. Grain Size Effects on Gas Sensitivity of Porous SnO_2-Based Elements. *Sens. Actuators, B* **1991**, *3*, 147−155.

(19) Yamazoe, N.; Fuchigami, J.; Kishikawa, M.; Seiyama, T. Interactions of Tin Oxide Surface with O_2, H_2O and H_2. *Surf. Sci.* **1979**, *86*, 335−344.

(20) Matsushima, S.; Teraoka, Y.; Miura, N.; Yamazoe, N. Electronic Interaction between Metal Additives and Tin Dioxide in Tin Dioxide-Based Gas Sensors. *Jpn. J. Appl. Phys.* **1988**, *27*, 1798−1802.

(21) Liewhirana, C.; Tamaekongb, N.; Wisitsoraatc, A.; Tuantranontc, A.; Phanichphant, S. Ultra-Sensitive H_2 Sensors Based on Flame-Spray-Made Pd-Loaded SnO_2 Sensing Films. *Sens. Actuators, B* **2013**, *176*, 893−905.

(22) Schweizer-Berberich, M.; Zheng, J. G.; Weimar, U.; Gopel, W.; Barsan, N.; Pentia, E.; Tomescu, A. The Effect of Pt and Pd Surface Doping on the Response of Nanocrystalline Tin Dioxide Gas Sensors to CO. *Sens. Actuators, B* **1996**, *31*, 71−75.

(23) Suematsu, K.; Shin, Y.; Hua, Z. Q.; Yoshida, K.; Yuasa, M.; Kida, T.; Shimanoe, K. Nanoparticle Cluster Gas Sensor: Controlled Clustering of SnO_2 Nanoparticles for Highly Sensitive Toluene Detection. *ACS Appl. Mater. Interfaces* **2014**, *6*, 5319−5326.

(24) Shimanoe, K.; Arisuda, S.; Oto, K.; Yamazoe, N. Influence of Reduction Treatment on CO Sensing Properties of SnO_2-Based Gas Sensor. *Electrochemistry* **2006**, *74*, 183−185.

DOI: 10.1021/am509082w
ACS Appl. Mater. Interfaces 2015, 7, 5863−5869